
Q-Rater: Non-Convex Optimization for Post-Training Uniform Quantization

Byeongwook Kim^{*1} Dongsoo Lee^{*1} Yeonju Ro¹ Yongkweon Jeon¹ Se Jung Kwon¹ Baeseong Park¹
Daehwan Oh¹

Abstract

Various post-training uniform quantization methods have usually been studied based on convex optimization. As a result, most previous ones rely on the quantization error minimization and/or quadratic approximations. Such approaches are computationally efficient and reasonable when a large number of quantization bits are employed. When the number of quantization bits is relatively low, however, non-convex optimization is unavoidable to improve model accuracy. In this paper, we propose a new post-training uniform quantization technique considering non-convexity. We empirically show that hyper-parameters for clipping and rounding of weights and activations can be explored by monitoring task loss. Then, an optimally searched set of hyper-parameters is frozen to proceed to the next layer such that an incremental non-convex optimization is enabled for post-training quantization. Throughout extensive experimental results using various models, our proposed technique presents higher model accuracy, especially for a low-bit quantization.

1. Introduction

The model size of deep neural networks (DNNs) is rapidly growing to support various complex target applications with increasing target accuracy goals. Hence, numerous model compression techniques are being actively studied to enable DNN inference operations for a given service response time while computing resources are limited. Such compression techniques include parameter pruning (Guo et al., 2016; Han et al., 2015), low-rank approximation (N. Sainath et al., 2013; Prabhavalkar et al., 2016), knowledge distillation (Hinton et al., 2015; Polino et al., 2018), and quantization (Courbariaux et al.,

2015; Hubara et al., 2016). In this paper, we discuss a quantization method specifically designed to preserve the model accuracy of DNNs.

Since quantization plays a major role to determine not only the (expensive) off-chip memory bandwidth but also the basic design principles of core arithmetic units performing DNN operations (Hubara et al., 2016; Lin et al., 2016), researchers are paying a lot of attention to the advance of DNN-dedicated quantization methods. For example, the Straight-Through Estimator (STE) (Courbariaux et al., 2015) is widely used for quantization-aware training to enable binary neural networks in which each weight and activation can be represented by one bit. In order to improve model accuracy after quantization, hyper-parameters for the quantization format can be designed to be differentiable and trainable (Jung et al., 2019; Khoram & Li, 2018; Zhu et al., 2017). Recently, even encryption techniques and training algorithms are introduced to implement sub-1-bit quantization with negligible accuracy drop (Lee et al., 2020). While quantization-aware training is effective to improve model accuracy, a wide range of post-training quantization schemes are also being considered because 1) DNN designers may not have enough expertise to consider model compression, and 2) model compression engineers may not be able to access the whole training dataset. As a result, numerous sophisticated post-training quantization algorithms are introduced (Wang et al., 2020; Zhao et al., 2019), and are being served by various DNN model development tools (Abadi et al., 2015; Paszke et al., 2019).

Most existing post-training quantization algorithms rely on convex-like optimization, essentially because fine-tuning or retraining as non-convex optimization is not available. For example, quantization errors on weights (Guo et al., 2017; Zhao et al., 2019; Zhou et al., 2017) or layer outputs (Nagel et al., 2017; Stock et al., 2019; Wang et al., 2020) are mainly minimized. When such minimization is NP-hard problems, quadratic approximations can be adopted to simplify the minimization process (Choi et al., 2017; Nagel et al., 2017). Note that when the amount of weight perturbation through quantization is large, then minimizing the quantization error may not be a convex-like optimization as shown in Figure 1. In addition, if a given loss surface of a pre-trained model is not smooth enough

^{*}Equal contribution ¹Samsung Research, Seoul, Republic of Korea. Correspondence to: Byeongwook Kim <byeongwook.kim@samsung.com >.

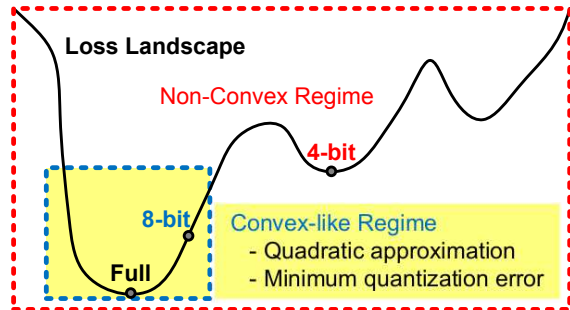


Figure 1. A loss landscape example where 8-bit quantization can be a convex-like optimization while optimal 4-bit quantization needs to be achieved by a non-convex optimization.

(Choromanska et al., 2015), then even post-training 8-bit quantization can be translated into a non-convex optimization problem. As a comprehensive post-training quantization, thus, an approach considering non-convexity is necessary.

Intuitively, it would be challenging to study a thorough non-convex analysis for post-training quantization. In this paper, based on the recognition that post-training inherently requires non-convex approaches, we propose a new post-training quantization method, called Q-Rater, that is especially useful for low-bit quantization. Instead of minimizing quantization errors, Q-Rater searches (not computes) hyper-parameters for quantization to minimize the task loss. The contributions in this paper can be summarized as follows:

- We present some examples suggesting that minimizing quantization error may not be tightly correlated with minimizing a training loss function.
- We propose new methods to find hyper-parameters determining clipping threshold values and rounding schemes. Such hyper-parameters are obtained by evaluating training loss function through a grid search for a layer. Then, searched hyper-parameters can be fixed for the next layer exploration.
- We show that bias correction needs to be selectively performed per layer.
- Experimental results describe that Q-Rater yields higher model accuracy compared to previous techniques relying on convex-like optimizations, especially when the number of quantization bits is low.

2. Weight quantization strategy

Let W and x represent weights and inputs of a layer, respectively. By large, post-training weight quantization

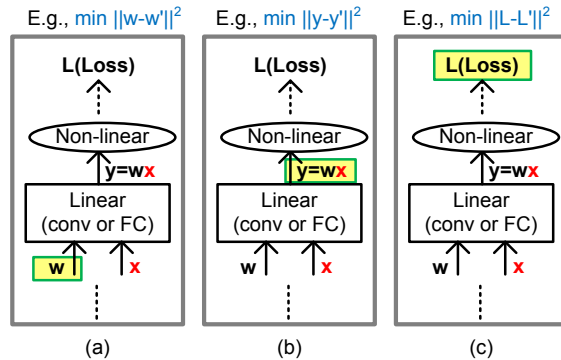


Figure 2. Comparison on three post-training quantization strategies. Quantization algorithm can be designed to minimize (a) quantization error on weights, (b) reconstruction error by quantization, or (c) task loss error by quantization.

strategies can be categorized into three schemes as shown in Figure 2 depending on the selection of the target variable to be minimized. Note that Figure 2(a) and 2(b) represent convex optimizations to calculate quantized W .

Weight only As the simplest method in Figure 2, weights can be quantized in a local optimization manner, i.e., weight quantization does not consider other layers nor activations. Various objective functions using the difference between W and quantized weights W' have been suggested. For example, the mean squared error (MSE) using a histogram (Shin et al., 2016) or a predetermined distribution model (Banner et al., 2019) can be minimized to obtain quantized weights. Minimizing KL divergence between full-precision weight distribution and quantized weight distribution is also proposed (Migacz, 2017). Since input data is not utilized, the quantization process can be simple and fast (Nagel et al., 2019) even though the correlation between weight quantization and task loss is not deeply investigated.

Layer output objective Given a specific domain of input data, quantized weights obtained only by using weights would not produce the best-quantized layer outputs (Stock et al., 2019). Correspondingly, to take into account the statistical properties of input domains, samples of inputs can be fed into the network and the quantization error on layer outputs can be minimized (Stock et al., 2019; Wang et al., 2020). Suppose that X is a set of input samples and the objective function is given as $\min \|WX - W'X'\|^2$. Then, compared to the case of Figure 2(a), the computational complexity (to solve $\min \|WX - W'X'\|^2$) may significantly increase because of large X . For example, feature size can be larger than the weight size in convolutional neural networks (CNNs) (He et al., 2016). In addition, the number of features (i.e., input sets) needs to

be much larger than 1. For instance, in the case of ResNet-101 on ImageNet, the number of elements in \mathbf{X} can be about 80M with 100 input samples (56x56 output size and 256 channels).

Task loss objective Weight quantization to produce the minimum task loss can be the most effective strategy if we find a sophisticated relationship between weight manipulation for quantization and corresponding task loss change. Unfortunately, because the task loss function of DNNs is non-convex (Goodfellow et al., 2016), there is no analytical solution to find the form of post-training quantized weights. As a result, various approximations are being suggested mainly by using quadratic approximations that imply quantization is performed in a convex-like regime (Nagel et al., 2017; Nahshan et al., 2020). Note that such approximations may hold only for a large number of quantization bits as we demonstrate in Section 4.

3. Activation quantization strategy

Unlike weights that can be quantized and fixed in advance, activations should be quantized on the fly during inference. In other words, weights are static data while activations are dynamic data that change during inference. Hence, quantization techniques dedicated to static data cannot be adopted for activation quantization. Accordingly, there are relatively fewer studies for activation (post-training) quantization compared to weight quantization. Thus, hyperparameters regarding activation quantization are usually drawn by a sampling of activations and estimating a distribution. For example, the moving average of activation values obtained by feeding input samples can be a clipping threshold (Jacob et al., 2018).

4. Issues on the previous methods

Some major issues on previous techniques for post-training quantization include that 1) non-convex properties are not exploited; 2) discussions on activations are somewhat overlooked; and 3) consequently, the impact of quantization on task loss is loosely coupled with an objective function to be minimized.

Let us first show that quantization needs to be considered as a non-convex optimization. When \mathbf{W}_{q1} and \mathbf{W}_{q2} are two quantized weights with different number of bits, interpolated \mathbf{W}_q is given as

$$\mathbf{W}_q = (1 - \alpha)\mathbf{W}_{q1} + \alpha\mathbf{W}_{q2}, \text{ for } \alpha \in [0, 1]. \quad (1)$$

Even though a thorough trajectory study between different parameter sets is highly complicated, evaluating a loss function $L(\mathbf{W}_q)$ with sweeping α can provide a 1-D interpolated trajectory cross-section to seek a counter-example

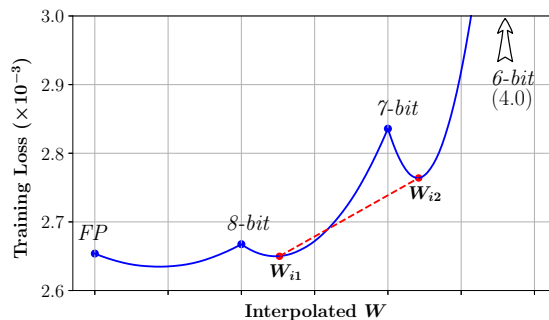


Figure 3. A simple 1-D trajectory investigation through interpolations of weight sets quantized from the same pre-trained ResNet-32 model on CIFAR-10.

of convex-like regime (Goodfellow et al., 2015). Figure 3 traces the training loss function when weight sets are interpolated using weights of full-precision or quantized. Note that if a function $f(x)$ is convex, then for any two points x_1 and x_2 , we obtain

$$f(\lambda x_1 + (1 - \lambda)x_2) \leq \lambda f(x_1) + (1 - \lambda)f(x_2), \quad (2)$$

when $\forall \lambda \in [0, 1]$. In Figure 3, we find that **training loss function is non-convex** because training loss value can be even lower when weight sets are interpolated such that Eq. 2 does not hold (e.g., training loss function is non-convex between \mathbf{W}_{i1} and \mathbf{W}_{i2} in Figure 3). Hence, Figure 3 supports our claim that convex-like optimizations could miss better quantization schemes.

Non-convexity of quantization can also be confirmed by investigating the relationship between quantization error and training loss. Suppose that n -bit quantization schemes lie in a convex-like regime. If it is the case, increasing quantization error would result in increasing training loss with a high correlation. As a case study, we apply 4-bit weight quantization to a few layers in ResNet-32 on CIFAR-10 using various quantization schemes that we discuss in the next section. Figure 4 illustrates that a correlation between quantization error (on weights) and training loss is not high such that low-bit quantization can be regarded as a non-convex problem. Similar observations are also reported in (Nagel et al., 2017; Stock et al., 2019) (where reconstruction error is minimized as a practical solution).

Analytical solutions based on the first two strategies in Figure 2 may not be appropriate for the post-training quantization of high non-convexity. In this work, we show that there is a way to find quantization schemes to reduce model accuracy reduction directly without quantization error minimization on weights or layer outputs.

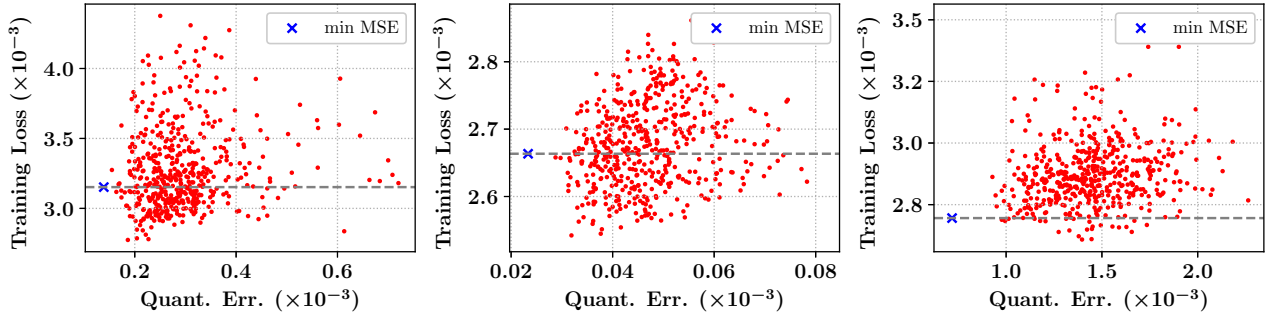


Figure 4. Correlation between quantization error and training loss of ResNet-32 (on CIFAR-10) when each weight of the 1st, the 16th, or the 31st layer is quantized by using 4 bits.

5. Q-Rater: holistic non-convex quantization

Unlike most previous methods proposing convex optimizations to obtain hyper-parameters for quantization, Q-Rater explores various hyper-parameters and evaluates corresponding training loss values using a grid search for a layer. Then, Bayesian optimization is performed to fine-tune a set of hyper-parameters in a layer. Once the fine-tuned hyper-parameters are achieved for a certain layer, then those hyper-parameters are frozen, and Q-Rater proceeds to the next target layer. For Q-Rater, we consider rounding and clipping as the underlying quantization operations. The bias correction method is also discussed in the context of non-convexity. In this section, Q-Rater operations (i.e., rounding, clipping, and bias correction) are individually introduced and then combined to present the overall impact on model accuracy.

Throughout this paper, even though Q-Rater does not rely on particular quantization formats, we assume **layer-wise** and **symmetric** quantization structure for both weights and activations. Such quantization structure is highly practical because 1) a floating-point scaling factor is shared by all elements in a layer, and thus, whole matrix multiplications (or convolutions) can be performed in fixed-point formats, and 2) computations for zero-point are not necessary (Jacob et al., 2018; Wang et al., 2020). We show that Q-Rater with such simple and computationally efficient quantization formats can maintain reasonable model accuracy for low-bit quantization.

5.1. Rounding scheme of Q-Rater

Assume that a (layer-wise) clipping threshold is given as $Th_c (> 0)$. As the first step of symmetric quantization, a weight is clipped to be $w_c = \max(\min(w, Th_c), -Th_c)$. Rounding is then performed to map a continuous value w_c into one of the discrete values that are pre-determined for uniform quantization. Note that rounding-to-nearest (RTN) has been dominating for uniform quantization since the per-

weight difference becomes the smallest after mapping. To be more specific, since we consider symmetric quantization, a scaling factor s is given as $s = Th_c / (2^{q-1} - 1)$ when q is the number of quantization bits. Then an integer w_r can be obtained by RTN as $w_r = \lfloor w_c / s + 0.5 \rfloor$. Training loss can be further reduced when weight is rounded up or down depending on the interaction between a perturbed weight and task loss. Recently proposed adaptive rounding, AdaRound (Nagel et al., 2017), investigates such an interaction using quadratic approximations and obtains rounding results by minimizing an asymmetric reconstruction formulation using gradient descent. The rounding principles of AdaRound, however, cannot be applied to activations since rounding needs to be a fixed hyper-parameter for each weight.

To allow rounding up and down for activations as well, Q-Rater takes into account (unequal) ranges of a variable to be quantized. In other words, Q-Rater divides a range of weights or activations into unequal parts where each part is mapped into the same discrete value. Specifically, we propose the two following rounding schemes to achieve a quantized weight w_q when $f_r(\cdot)$ decides the rounding (activations follow the same procedures).

1st-order rounding scheme (γ_n):

$$w_q = s \cdot \left\lfloor \frac{w_c}{s} + 0.5 + f_r(w_c, \gamma_n) \right\rfloor, \quad (3)$$

$$f_r(w_c, \gamma_n) = 0.5 \cdot \text{sign}(w_c \gamma_n) \cdot |\gamma_n|^{|w_r|}, \quad (4)$$

where $\gamma_n \in [-1, 1]$ is a hyper-parameter. If $\gamma_n = 0$, Eq. 3 is equivalent to RTN.

2nd-order rounding scheme (γ_n, γ_s):

$$w_q = s \cdot \left\lfloor \frac{w_c}{s} + 0.5 + f_r(w_c, \gamma_n, \gamma_s) \right\rfloor, \quad (5)$$

$$f_r(w_c, \gamma_n, \gamma_s) = 0.5 \cdot \text{sign}(w_c \gamma_n (\gamma_s \cdot 2^{q-1} - |w_r|)) \cdot |\gamma_n|^{\left| |w_r| - \gamma_s \cdot 2^{q-1} - \beta \right|}, \quad (6)$$

where $\beta = 2^{q-2}$, and $\gamma_n \in [-1, 1]$ and $\gamma_s \in [0, 1]$ are hyper-parameters. $\gamma_n = 0$ produces RTN regardless of γ_s .

The proposed rounding scheme is illustrated in Figure 5 (due to the space limit, all illustrations about 1st-order rounding are provided in Appendix A). Since $f_r(\cdot)$ has the range of $[-0.5, 0.5]$ for both proposed 1st- and 2nd-order round schemes, Eq. 3 and 5 can select one of three rounding schemes, namely, RTN, round up, and round down. γ_n controls the amount of inequality among mapping ranges while γ_s (for 2nd-order rounding) decides from where mapping ranges start to increase or decrease.

Now let us explain how to find hyper-parameters for rounding. First, for a target layer, we find a clipping threshold Th_c . Then, we sweep γ_n and γ_s , and find a particular set of γ_n and γ_s that correspond to the best training loss. Once the optimal γ_n and γ_s are obtained through such a grid search, then we quantize the weights of a target layer. Those quantized weights are fixed and we proceed to the next layer.

We apply different rounding methods to activations and/or weights of the ResNet-32 model on CIFAR-10 while quantization is performed incrementally from the second layer to the last one (note that the first layer is too small in ResNet-32). To be focused on the impact of the new rounding scheme, we utilize MSE minimization to compute the clipping threshold Th_c as verified to be effective in (Zhao et al., 2019) while we propose a new clipping technique in the next subsection. Sweep interval is 0.1 for both γ_n and γ_s . Figure 6 compares quantization results of ResNet-32 model on CIFAR-10 using RTN or 2nd-order Q-Rater rounding scheme ($q = 3$ for both weights and activations). When $\gamma_s = 0.2$, sweeping γ_n to quantize the weights of the 31st layer yields high variations on train accuracy. Note that for both weights and activations, RTN (i.e., $\gamma_n = 0$) does not provide the best train accuracy and the optimal γ_n is far from zero. A set of γ_n values optimized separately for each layer leads to significantly improved test accuracy as layers are quantized incrementally as shown on the left of Figure 6. For the experimental results using ResNet-18 and MobileNetV2 on ImageNet (with only 20K input samples), refer to Appendix A. Throughout comprehensive experiments, the 2nd-order rounding scheme offers slightly better results than the 1st-order rounding scheme (shown in Appendix A). For the remainder of this paper, thus, we choose the 2nd-order rounding scheme.

5.2. Clipping method of Q-Rater

Most DNN models exhibit a bell-shaped distribution for weights and activations (Zhao et al., 2019). Hence, a few outliers in distribution can affect the overall quality of

uniform quantization decisively. Clipping method, therefore, is being widely used for post-training quantization (Banner et al., 2019; Jacob et al., 2018; Zhao et al., 2019) as a trade-off between the quantization resolution and the amount of outliers’ quantization error.

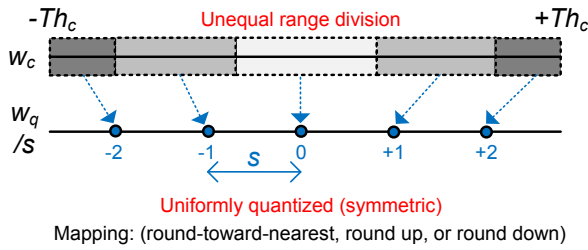
Recently proposed clipping methods include MSE minimization (i.e., L2-norm between the full-precision values and quantized values is minimized (Shin et al., 2016; Sung et al., 2016)), ACIQ (i.e., minimizing MSE between a pre-determined distribution model and the full-precision model (Banner et al., 2019)), and KL divergence minimization (Migacz, 2017). An additional method to control outliers is outlier channel splitting (OCS) that duplicates channels containing outliers, and then halves activations or weights without modifying the functionality of a model (Zhao et al., 2019). OCS becomes more effective when combined with existing clipping methods (Zhao et al., 2019). Note that non-convexity is not recognized for those previous clipping techniques.

For Q-Rater, we introduce a hyper-parameter $\gamma_c \in (0.0, 1.0)$ to determine $Th_c = \max(\mathbf{W}) \cdot \gamma_c$ when $\max(\mathbf{W})$ describes the maximum elements of a set of full-precision weights \mathbf{W} (clipping for activations follows the same structure). Similar to our rounding schemes, we sweep γ_c from 0 to 1 and investigate the corresponding training accuracy. For experiments, after an optimal γ_c (producing the best training accuracy) is obtained through a sweeping, RTN is followed for each weight and activation (RTN is used to study the impact of clipping method independently). We perform an incremental quantization and Figure 7 presents the results using the ResNet-32 model on CIFAR-10 with different clipping methods. It is clear that for low-bit quantization (e.g., $q = 3$ in Figure 7), conventional techniques may not produce the best training accuracy. When such γ_c optimization for a layer is conducted incrementally through all target layers, Q-Rater presents significantly higher test accuracy compared to MSE, ACIQ, and KL. Experimental results using the ResNet-18 model on ImageNet are presented in Appendix B.

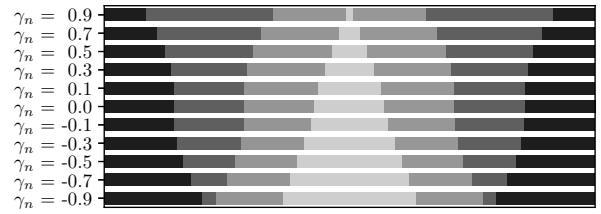
5.3. Bias correction of Q-Rater

Bias correction is an operation to compensate for the biased error in output activations after quantization. The amount of shift induced by quantization is diminished by adjusting the bias parameters of the neurons or channels because shifted output activations through quantization may degrade the quantization quality of the next layer (Finkelstein et al., 2019; Nagel et al., 2019). The amount of shift can be calculated as the expected error on the output activations that can be expressed as

$$\mathbb{E}[\mathbf{y}] - \mathbb{E}[\mathbf{y}'] = \mathbb{E}[\mathbf{W}\mathbf{X}] - \mathbb{E}[\mathbf{W}'\mathbf{X}']. \quad (7)$$



(a) Proposed mapping method by unequal range division of a weight or activation.



(b) Examples of unequal range division by 2nd-order rounding scheme when $\gamma_s = 0.5$ with various γ_n .

Figure 5. Proposed rounding scheme based on unequally divided ranges to be mapped to quantized values.

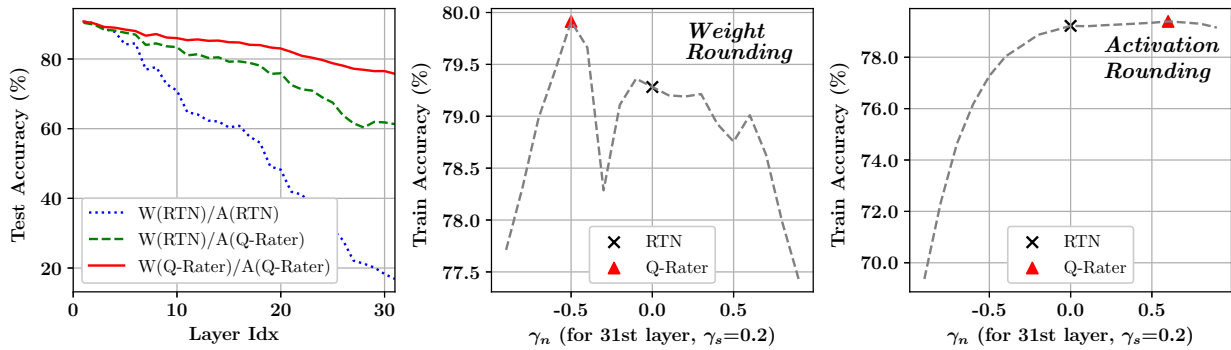


Figure 6. Test accuracy comparison using ResNet-32 model (on CIFAR-10) when weights and/or activations are rounded by RTN or the proposed (2nd-order) rounding scheme that evaluates train accuracy with various γ_n and γ_s . 3-bit quantization is performed from the second layer to the last one incrementally and the clipping method follows MSE minimization.

Then, the expected error (or shift) of the output activations is subtracted from the corresponding layer’s bias terms.

Bias correction has been a supplementary and optional technique for quantization. For example, bias correction is not introduced in (Zhao et al., 2019) while it is playing a key role in enhancing model accuracy in (Finkelstein et al., 2019; Nagel et al., 2019). In the context of non-convexity, Q-Rater compares two model accuracy values evaluated with or without bias correction for a layer. Only when bias correction turns out to improve model accuracy for a given layer, Q-Rater compensates for bias terms of output activations. Such selective application of bias correction implies that reducing quantization error on layer outputs (described in Figure 2) may not reduce model accuracy drop.

Figure 8 presents incremental quantization results using ResNet-32 on CIFAR-10 with different bias correction schemes (when weights and activations are quantized by using RTN and MSE clipping). When combined with RTN and MSE clipping, bias correction is effective for initial layers in Figure 8. Then, model accuracy is dropped sharply for a few final layers. On the other hand, interestingly, selective bias correction by Q-Rater offers significantly improved test accuracy throughout the entire layers.

Hence, searching for quantization schemes differently for each layer based on training accuracy monitoring is effective for bias correction as well. Interestingly, as shown in Appendix C, more layers require bias correction as q decreases while the locations of such layers seem to be random. It is also interesting that MobileNetV2 demands bias corrections for layers close to inputs and outputs. Refer to Appendix C for experimental results using ResNet-18 and MobileNetV2 on ImageNet.

5.4. Combination effects on Q-Rater operations

So far, we studied Q-Rater operations (i.e., rounding, clipping, and bias correction) individually. Now, we combine those Q-Rater operations to see combination effects. For experiments, as a reference quantization scheme, weights and activations are quantized by using RTN and MSE-based clipping without bias correction. Then each quantization operation is replaced with that of Q-Rater. We perform a grid search to find $\gamma_n \in [-1, 1]$, $\gamma_s \in [0, 1]$, and $\gamma_c \in [0, 1]$ (by monitoring training task loss) when the search resolutions are 0.1, 0.25, and 0.1, respectively. The entire Q-Rater procedures are described in Algorithm 1 (Appendix E). When Q-Rater operations are combined, clipping is performed first and rounding is followed. After

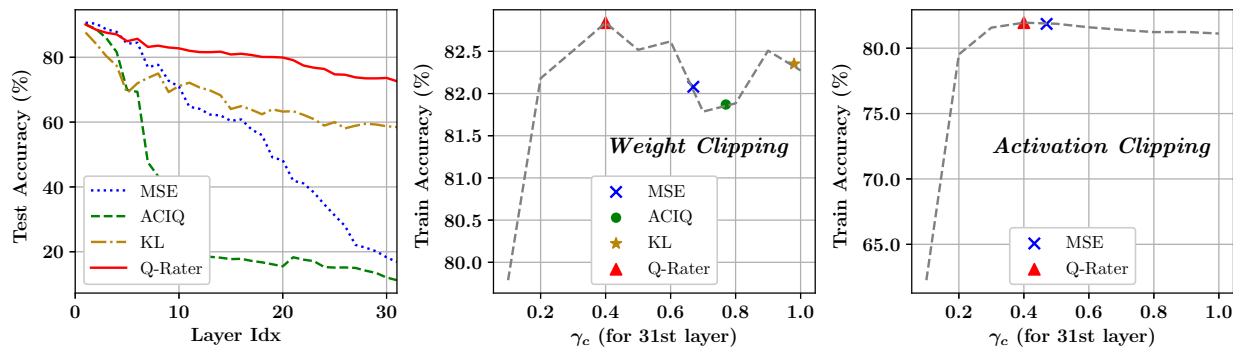


Figure 7. Test accuracy comparison using MSE, ACIQ, KL, or our proposed clipping method with RTN rounding scheme for weights and activations of ResNet-32 model on CIFAR-10 ($q = 3$ for both weights and activations). For each layer, Q-Rater sweeps γ_c and evaluates corresponding train accuracy.

Table 1. Top-1 test accuracy (%) of various models quantized by previous methods or by Q-Rater. Model names are annotated with dataset and test accuracy of full-precision. All results are accompanied by **layer-wise** and **symmetric** quantization.

Model	W/A bits	Clip (+RTN) ¹			Q-Rater (Proposed)				
		MSE	ACIQ	KL	①(Round) ²	②(Clip)	③(Bias)	①+②	①+②+③
ResNet-32	5/5	90.64	75.68	90.45	91.70	91.68	91.64	91.93	91.74
<i>on CIFAR-10</i>	4/4	84.46	24.57	71.32	89.03	89.60	88.47	89.71	90.24
(92.63)	3/3	16.86	11.23	58.48	75.74	72.61	67.63	77.35	79.69
ResNet-18	8/8	69.25	68.15	68.39	69.27	69.35	69.50	69.33	69.43
<i>on ImageNet</i>	6/6	66.75	59.78	65.64	67.34	67.91	67.42	67.95	68.46
(69.69)	4/4	32.16	2.10	11.27	45.18	52.59	51.59	54.87	59.17
MobileNetV2	8/8	69.81	69.98	69.98	71.01	70.73	71.34	70.92	71.25
<i>on ImageNet</i>	6/6	36.82	11.08	38.63	64.15	61.04	64.89	65.33	67.64
(71.78)	4/4	0.12	0.39	0.22	7.08	4.67	6.58	15.58	25.35

¹ Reference code: <https://github.com/cornell-zhang/dnn-quant-ocs>

² 2nd-order rounding scheme is applied.

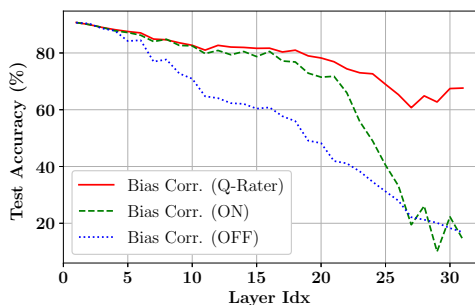


Figure 8. Test accuracy of ResNet-32 model on CIFAR-10 when bias correction is always applied, never applied, or selectively applied by Q-Rater. Weights and activations are quantized (by using $q = 3$) incrementally with RTN and MSE clipping.

weights and activations are quantized by γ_n, γ_s , and γ_c , selective bias correction for Q-Rater is conducted. Note that we restrict our interests to layer-wise and symmetric quantization that is efficient for inference but challenging in terms of maintaining test accuracy. In the case of the ImageNet dataset, we choose 20K samples only for fast evaluations of the model.

Table 1 presents top-1 test accuracy of ResNet-32 (on CIFAR-10), ResNet-18 (on ImageNet), and MobileNetV2 (on ImageNet) when quantized by selected previous methods and by Q-Rater. Previous methods include three different clipping methods (i.e., MSE, ACIQ, and KL) and RTN without bias correction (as introduced in (Zhao et al., 2019)). Note that all three individual Q-Rater operations outperform previous methods. We also observe that combining multiple Q-Rater operations can substantially improve test accuracy for low-bit quantization.

6. Experimental results

The success of Q-Rater largely depends on the search quality of hyper-parameters γ_n, γ_s , and γ_c . Even though a

Table 2. Top-1 test accuracy (%) comparison results. Q-Rater performs clipping (using γ_c), rounding (2nd-order using γ_n and γ_s), and selective bias correction sequentially for a layer.

Dataset	Model (Full Acc.)	W/A bits	MSE	OCS ¹ (+MSE)	Bit-Split ²	Q-Rater (●+●+●)	
						Grid Search	Bayesian Opt.
ImageNet	ResNet-18 (69.69)	8/8	69.31	69.38	69.48	69.43	69.67
		6/6	66.75	67.51	68.59	68.46	68.60
		4/4	32.16	34.85	55.18	59.17	60.77
	ResNet-101 (77.79)	8/8	77.02	77.18	77.20	77.10	77.16
		6/6	74.20	75.36	0.08 ³	75.97	76.21
		4/4	19.48	29.76	0.06 ³	64.49	68.24
MobileNetV2 (71.78)	8/8	69.81	N/A	70.60 ⁴	71.25	71.10	
	6/6	36.82	N/A	53.88 ⁴	67.64	68.20	
	4/4	0.12	N/A	0.28 ⁴	25.35	22.95	
CIFAR-10	ResNet-32 (92.63)	5/5	90.64	91.14	91.68	91.74	91.84
		4/4	84.46	86.87	89.50	90.24	90.15
		3/3	16.86	35.97	76.07	79.69	79.71

¹ Reference code: <https://github.com/cornell-zhang/dnn-quant-ocs>

² Reference code: <https://github.com/wps712/BitSplit>

³ Numerical instability is observed probably because of matrices of too large dimensions.

⁴ While depthwise convolution is not discussed in the reference, for our experiments, we revise the reference code such that depthwise convolution layers are quantized in a way to quantize fully-connected layers.

coarse-grained grid search method can produce impressive results as shown in Table 1, as a way of fine-tuning hyper-parameters, we adopt Bayesian Optimization¹ (BO), one of the automated techniques to search parameter spaces. After a brief introduction of the BO technique, we introduce the outlier channel split (OCS) (Zhao et al., 2019) and bit-split (Wang et al., 2020) as examples minimizing quantization error on weights and layer outputs, respectively. Then, we show comparison results on model accuracy.

Bayesian optimization For a given dataset D and a given parameter vector $\mathbf{h}=\{\gamma_c\}$ or $\mathbf{h}=\{\gamma_n, \gamma_s\}$, BO aims to find an optimal \mathbf{h}^* which maximizes an evaluation function $f(\mathbf{h}, D)$ for a network. Four times processes for each layer are required in our suggested algorithm (refer to Algorithm 1 in Appendix). To avoid over-fitting of quantization parameters to a test dataset, a training dataset or a subset of the training dataset is used for evaluation at each step. Using grid search results as initial search space, in our experiments, BO explores additional 50 hyper-parameter sets.

Outlier channel split OCS represents recent efforts to minimize quantization error on weights. Halved outliers in weights due to OCS without model structure modifications enable aggressive clipping that plays a pivotal role in uniform quantization. It is reported that OCS improves MSE, ACIQ, and KL-based clipping noticeably especially for low-bit quantization of weights (Zhao et al., 2019).

Bit-split We introduce the bit-split technique as one of the attempts to minimize reconstruction error (i.e., quantization error on layer outputs) for post-training uniform quantization. Bit-split formulates quantization as an optimization problem where quantization-related parameters are computed in an iterative fashion to solve a complicated objective function. While partial analytical solutions are obtained during iterative procedures, matrix multiplications can entail large \mathbf{X} matrices whose dimensions increase with the number of input samples and the size of input features.

Comparison results Table 2 presents comparison results on top-1 test accuracy of ResNet-18, ResNet-101 (representing large depth models), and MobileNetV2 (challenging to be quantized mainly due to depth-wise layers) on ImageNet dataset, and ResNet-32 on CIFAR-10 dataset. **For ImageNet, Q-Rater does not need the entire dataset.** Instead, we use only 20K random samples to estimate the loss function (see Appendix D for the relationship between the number of samples and quantization quality). For Q-Rater with grid search, we use the same search resolutions of the previous section (i.e., 0.1 for γ_n , 0.25 for γ_s , and 0.1 for γ_c). We observe that even for layer-wise and symmetric quantization we choose for this work, OCS indeed enhances MSE. Then, bit-split outperforms OCS except for the ResNet-101 model where we observe numerical instability during computations (probably because of too complicated analytical equations that can be potentially solved by higher precision such as double precision). Note that since we assume layer-wise quantization, bit-split entails a lot more complicated computations compared to channel-wise quantization that

¹We use a publicly available code in (Nogueira, 2014–).

is chosen in (Wang et al., 2020). For all models in the table, Q-Rater presents the best test accuracy while BO slightly exceeds a grid search for most cases.

7. Conclusion

In this paper, we propose a new post-training uniform quantization technique, called Q-Rater, which does not depend on convex optimizations. While previous works mainly compute hyper-parameters for quantization to minimize quantization errors on weights or layer outputs, we suggest that we can perform a grid search of quantization hyper-parameters by evaluating corresponding training loss. For each layer, hyper-parameters for clipping and rounding are searched, and then bias correction is conducted selectively. Through layer-wise incremental optimization for hyper-parameters, Q-Rater presents significantly higher model accuracy for various CNN models even assuming a simple layer-wise and symmetric quantization format.

References

- Abadi, M., Agarwal, A., Barham, P., Brevdo, E., Chen, Z., Citro, C., Corrado, G. S., Davis, A., Dean, J., Devin, M., Ghemawat, S., Goodfellow, I., Harp, A., Irving, G., Isard, M., Jia, Y., Jozefowicz, R., Kaiser, L., Kudlur, M., Levenberg, J., Mané, D., Monga, R., Moore, S., Murray, D., Olah, C., Schuster, M., Shlens, J., Steiner, B., Sutskever, I., Talwar, K., Tucker, P., Vanhoucke, V., Vasudevan, V., Viégas, F., Vinyals, O., Warden, P., Wattenberg, M., Wicke, M., Yu, Y., and Zheng, X. TensorFlow: Large-scale machine learning on heterogeneous systems, 2015. URL <https://www.tensorflow.org/>. Software available from tensorflow.org.
- Banner, R., Nahshan, Y., Hoffer, E., and Soudry, D. Post-training 4-bit quantization of convolution networks for rapid-deployment. *arXiv:1810.05723*, 2019.
- Choi, Y., El-Khamy, M., and Lee, J. Towards the limit of network quantization. In *International Conference on Learning Representations (ICLR)*, 2017.
- Choromanska, A., Henaff, M., Mathieu, M., Arous, G. B., and LeCun, Y. The loss surfaces of multilayer networks. In *Proceedings of the Eighteenth International Conference on Artificial Intelligence and Statistics, AISTATS*, 2015.
- Courbariaux, M., Bengio, Y., and David, J.-P. BinaryConnect: Training deep neural networks with binary weights during propagations. In *Advances in Neural Information Processing Systems*, pp. 3123–3131, 2015.
- Finkelstein, A., Almog, U., and Grobman, M. Fighting quantization bias with bias. *arXiv:1906.03193*, 2019.
- Goodfellow, I., Bengio, Y., and Courville, A. *Deep Learning*. MIT Press, 2016. <http://www.deeplearningbook.org>.
- Goodfellow, I. J., Vinyals, O., and Saxe, A. M. Qualitatively characterizing neural network optimization problems. *arXiv:1412.6544*, 2015.
- Guo, Y., Yao, A., and Chen, Y. Dynamic network surgery for efficient DNNs. In *Advances in Neural Information Processing Systems*, 2016.
- Guo, Y., Yao, A., Zhao, H., and Chen, Y. Network sketching: exploiting binary structure in deep CNNs. In *IEEE Conference on Computer Vision and Pattern Recognition (CVPR)*, pp. 4040–4048, 2017.
- Han, S., Pool, J., Tran, J., and Dally, W. J. Learning both weights and connections for efficient neural networks. In *Advances in Neural Information Processing Systems*, pp. 1135–1143, 2015.
- He, K., Zhang, X., Ren, S., and Sun, J. Deep residual learning for image recognition. *2016 IEEE Conference on Computer Vision and Pattern Recognition (CVPR)*, pp. 770–778, 2016.
- Hinton, G., Vinyals, O., and Dean, J. Distilling the knowledge in a neural network. In *NIPS Deep Learning and Representation Learning Workshop*, 2015.
- Hubara, I., Courbariaux, M., Soudry, D., El-Yaniv, R., and Bengio, Y. Quantized neural networks: training neural networks with low precision weights and activations. *arXiv:1609.07061*, 2016.
- Jacob, B., Kligys, S., Chen, B., Zhu, M., Tang, M., Howard, A., Adam, H., and Kalenichenko, D. Quantization and training of neural networks for efficient integer-arithmetic-only inference. In *Proceedings of the IEEE Conference on Computer Vision and Pattern Recognition*, pp. 2704–2713, 2018.
- Jung, S., Son, C., Lee, S., Son, J., Kwak, Y., Han, J.-J., Hwang, S. J., and Choi, C. Learning to quantize deep networks by optimizing quantization intervals with task loss. In *IEEE Conference on Computer Vision and Pattern Recognition (CVPR)*, pp. 4350–4359, 2019.
- Khoram, S. and Li, J. Adaptive quantization of neural networks. In *International Conference on Learning Representations (ICLR)*, 2018.
- Lee, D., Kwon, S. J., Kim, B., Jeon, Y., Park, B., and Yun, J. FlexOR: trainable fractional quantization. In *Advances in Neural Information Processing Systems*, 2020.

- Lin, D., Talathi, S., and Annapureddy, S. Fixed point quantization of deep convolutional networks. In *International Conference on Machine Learning*, pp. 2849–2858, 2016.
- Migacz, S. 8-bit inference with TensorRT. In *NVIDIA GPU Technology conference*, 2017.
- N. Sainath, T., Kingsbury, B., Sindhvani, V., Arisoy, E., and Ramabhadran, B. Low-rank matrix factorization for deep neural network training with high-dimensional output targets. In *ICASSP*, pp. 6655–6659, 2013.
- Nagel, M., Amjad, R. A., van Baalen, M., Louizos, C., and Blankevoort, T. Up or down? adaptive rounding for post-training quantization. In *International Conference on Machine Learning (ICML)*, pp. 7696–7705, 2017.
- Nagel, M., van Baalen, M., Blankevoort, T., and Welling, M. Data-free quantization through weight equalization and bias correction. *arXiv:1906.04721*, 2019.
- Nahshan, Y., Chmiel, B., Baskin, C., Zheltonozhskii, E., Banner, R., Bronstein, A. M., and Mendelson, A. Loss aware post-training quantization. *arXiv:1911.07190*, 2020.
- Nogueira, F. Bayesian Optimization: Open source constrained global optimization tool for Python, 2014–. URL <https://github.com/fmfn/BayesianOptimization>.
- Paszke, A., Gross, S., Massa, F., Lerer, A., Bradbury, J., Chanan, G., Killeen, T., Lin, Z., Gimelshein, N., Antiga, L., Desmaison, A., Kopf, A., Yang, E., DeVito, Z., Raison, M., Tejani, A., Chilamkurthy, S., Steiner, B., Fang, L., Bai, J., and Chintala, S. Pytorch: An imperative style, high-performance deep learning library. In *Advances in Neural Information Processing Systems 32*, pp. 8024–8035. 2019.
- Polino, A., Pascanu, R., and Alistarh, D. Model compression via distillation and quantization. In *International Conference on Learning Representations (ICLR)*, 2018.
- Prabhavalkar, R., Alsharif, O., Bruguier, A., and McGraw, I. On the compression of recurrent neural networks with an application to LVCSR acoustic modeling for embedded speech recognition. In *ICASSP*, pp. 5970–5974, 2016.
- Shin, S., Hwang, K., and Sung, W. Fixed-point performance analysis of recurrent neural networks. In *2016 IEEE International Conference on Acoustics, Speech and Signal Processing (ICASSP)*, pp. 976–980, 2016.
- Stock, P., Joulin, A., Gribonval, R., Graham, B., and Jégou, H. And the bit goes down: Revisiting the quantization of neural networks. *arXiv:1907.05686*, 2019.
- Sung, W., Shin, S., and Hwang, K. Resiliency of deep neural networks under quantization. *arXiv:1511.06488*, 2016.
- Wang, P., Chen, Q., He, X., and Cheng, J. Towards accurate post-training network quantization via bit-split and stitching. In *International Conference on Machine Learning (ICML)*, pp. 243–252, 2020.
- Zhao, R., Hu, Y., Dotzel, J., Sa, C. D., and Zhang, Z. Improving neural network quantization without retraining using outlier channel splitting. In *International Conference on Machine Learning (ICML)*, pp. 7543–7552, 2019.
- Zhou, S., Wang, Y., Wen, H., He, Q., and Zou, Y. Balanced quantization: An effective and efficient approach to quantized neural networks. *Journal of Computer Science and Technology*, 32:667–682, 2017.
- Zhu, C., Han, S., Mao, H., and Dally, W. J. Trained ternary quantization. In *International Conference on Learning Representations (ICLR)*, 2017.

A. Evaluation of Q-Rater Rounding Scheme

In this section, we provide comprehensive experimental results to demonstrate the effectiveness of the proposed Q-rater rounding scheme. We show how the 1st-order and the 2nd-order Q-rater rounding methods divide the entire range by using different γ_n . And then, we evaluate the proposed scheme on various models. For the evaluation, pre-trained ResNet32 on CIFAR-10 dataset, ResNet18 and MobileNetV2 on ImageNet dataset are used. We present the experimental results of the 1st-order and the 2nd-order rounding schemes.

A.1. Q-Rater Range Division Examples

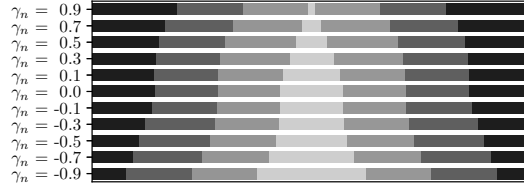


Figure 9. Examples of unequal range division by the 1st-order rounding scheme with various γ_n .

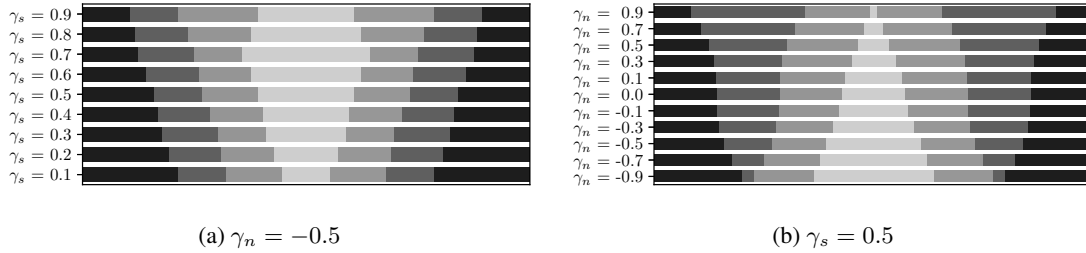


Figure 10. Examples of unequal range division by the 2nd-order rounding scheme with various γ_n and γ_s .

Figure 9 and Figure 10 show how the range is divided by the 1st-order and the 2nd-order Q-Rater rounding. If γ_n is zero, then Q-Rater is exactly the same as the conventional Rounding-to-Nearest (RTN) scheme in both cases. With the 1st-order Q-Rater rounding, the size of range monotonically increases or decreases from the zero. For example, the range always decreases as it goes further away from the zero when $\gamma_n > 0$. Meanwhile, the range always increases as it goes further away from the zero when $\gamma_n < 0$. With the 2nd-order Q-Rater rounding, γ_s decides where to start increase or decrease.

A.2. ResNet-32 on CIFAR-10

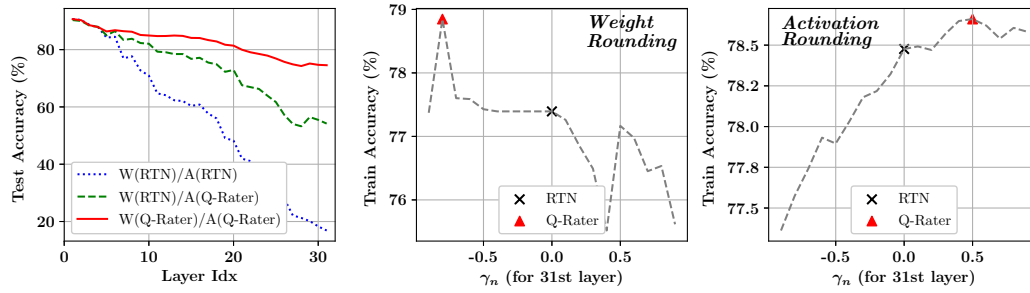


Figure 11. Comparison between Rounding-to-Nearest (RTN) and the 1st-order Q-Rater rounding. 3-bit quantization is performed from the second layer to the last layer. MSE minimization is used for the clipping method.

Figure 11 compares the Rounding-to-Nearest (RTN) scheme and the 1st-order Q-Rater rounding scheme using ResNet32. As quantization is performed incrementally per layer, test accuracy continues to drop for both quantization schemes. Note that Q-Rater rounding yields less accuracy drop compared to the RTN throughout layers. It is more effective when Q-Rater is applied to both the weights and activation, though the case when Q-Rater is applied to the activations only also outperforms the RTN. The second and the third plots show train accuracy by different γ_n values used in the weight rounding and the activation rounding, respectively. If γ_n is 0.0, the result is the same as the RTN. Those two plots with various γ_n indicate that the RTN does not guarantee the best accuracy and there exist opportunities to find other parameters that provide better accuracy. The 1st-order Q-Rater rounding scheme searches a particular γ_n that exhibits the best training accuracy.

A.3. ResNet-18 on ImageNet

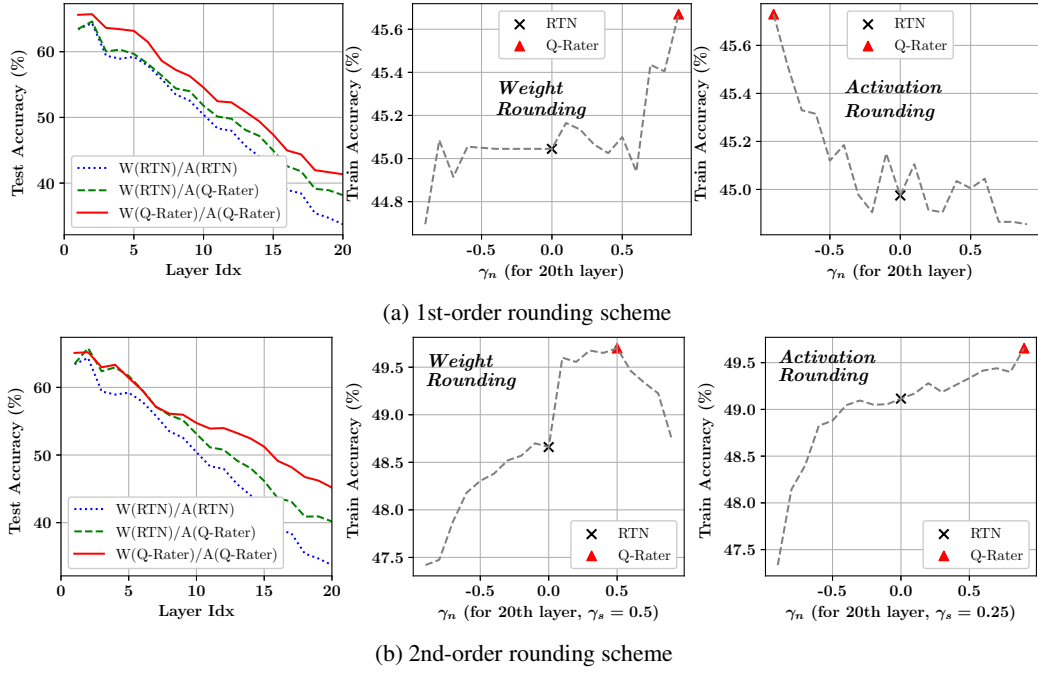


Figure 12. Comparison of Rounding-to-Nearest(RTN) and the 1st-order and the 2nd-order Q-Rater. 4-bit quantization is performed to all layers including the first and the last layer. MSE minimization is used for the clipping method.

Figure 12 compares the Rounding-to-Nearest (RTN) scheme and the 1st-order and the 2nd-order Q-Rater rounding scheme in ResNet-18. The ResNet-18 model used in the quantization is trained by using the ImageNet dataset. As illustrated in Figure 11, Q-Rater is more tolerant to the accuracy drop by quantization compared to the RTN. Specifically, Q-Rater shows the best performance when the 2nd-order rounding scheme is applied to both the weights and the activations. The second and the third plots in Figure 12(a) and (b) show train accuracy by different γ_n . For the 2nd-order rounding scheme, γ_s is fixed to the value depicted in the figure. As shown in the figure, train accuracy varies by γ_n , and RTN does not necessarily result in the best train accuracy for both weight rounding and activation rounding. By estimating train accuracy, Q-Rater finds γ_n and γ_s to achieve the best accuracy.

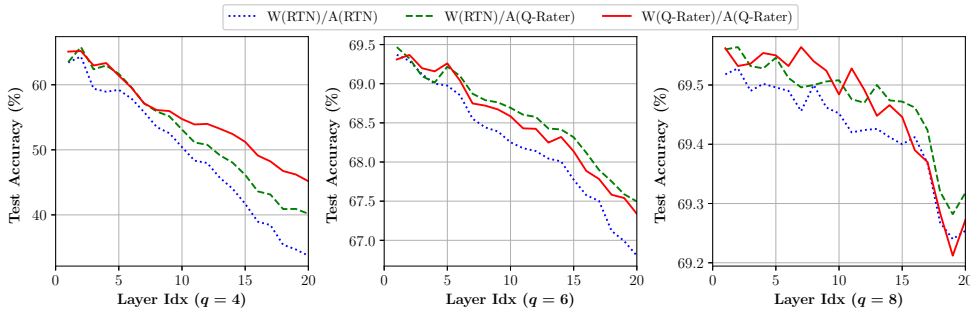


Figure 13. Comparison of Rounding-to-Nearest (RTN) and the 2nd-order Q-Rater by using the different number of quantization bits. Quantization is performed from the second to the last layer. MSE minimization is used for the clipping.

Figure 13 compares the Rounding-to-Nearest (RTN) scheme and the 2nd-order Q-Rater rounding scheme using the ResNet18 model. From left to right, $q = 4$, $q = 6$, or $q = 8$ is used to quantize the weights and the activations. With 8-bit quantization, both RTN and Q-Rater show nearly full accuracy. In the case of 6-bit quantization, the difference between W(RTN)/A(Q-Rater) and W(Q-Rater)/A(Q-Rater) is less than 0.1%. When $q = 4$ is used as a more extreme environment, W(Q-Rater)/A(Q-Rater) significantly outperforms the conventional RTN scheme.

A.4. MobileNetV2 on ImageNet

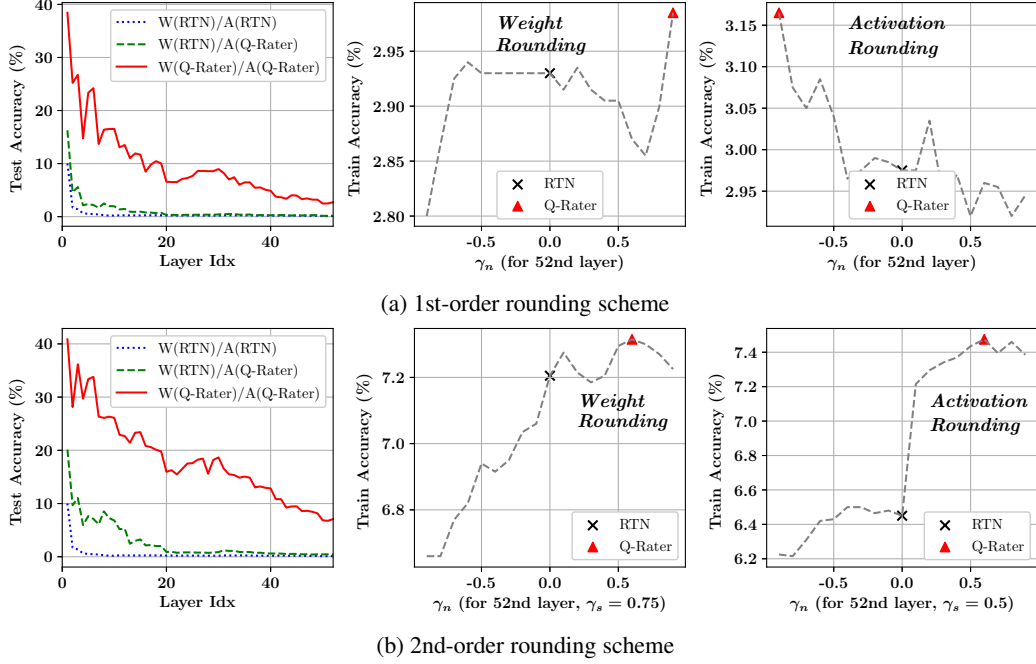


Figure 14. Comparison of Rounding-to-Nearest (RTN) and the 1st-order and the 2nd-order Q-Rater. 4-bit quantization is performed from the second to the last layer. MSE minimization is used for the clipping method.

Figure 14 compares the Rounding-to-Nearest (RTN) scheme and the 1st-order and the 2nd-order Q-Rater rounding scheme using MobileNetV2, trained on the ImageNet dataset. Similar to our observations on other models, Q-Rater is more tolerant in the accuracy drop by quantization compared to the RTN, and it shows the best performance when the 2nd-order rounding scheme is applied to both the weights and the activations. The second and the third plots in Figure 14(a) and (b) show train accuracy by different γ_n . For the 2nd-order rounding scheme, γ_s is fixed to the value depicted in the figure. As shown in the figure, train accuracy varies by γ_n and RTN does not necessarily result in the best train accuracy in both cases. Depending on the measured train accuracy, Q-Rater finds γ_n and γ_s to achieve the best accuracy.

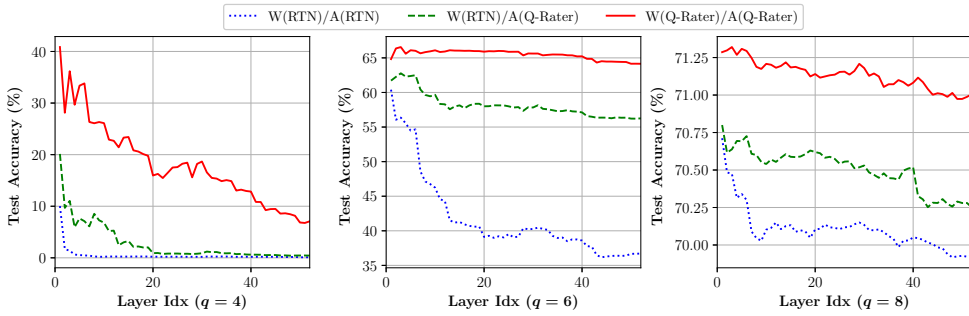


Figure 15. Comparison of Rounding-to-Nearest (RTN) and the 2nd-order Q-Rater by using the different number of quantization bits. Quantization is performed from the second to the last layer. MSE minimization is used for the clipping.

Figure 15 compares the Rounding-to-Nearest (RTN) scheme and the 2nd-order Q-Rater rounding scheme in the MobileNetV2 model. From left to right, $q = 4$, $q = 6$, or $q = 8$ is used to quantize the weights and the activations. For 8-bit quantization, W(Q-Rater)/A(Q-Rater) shows improvement over the others and produces nearly full accuracy while other schemes do not. In the case of 6-bit quantization, Q-Rater significantly improves the accuracy even in the case when Q-Rater is applied only to the activations. When $q = 4$ is used as a more extreme environment, W(Q-Rater)/A(Q-Rater) outperforms the conventional RTN scheme as well.

A.5. Comparison of the 1st order and 2nd order schemes.

Table 3. Comparison of top-1 accuracy (%) with the proposed Q-Rater.

Dataset	Model	W/A	1st-order			2nd-order		
			1 ¹	1+2 ³	1+2+3 ⁴	1 ²	1+2 ³	1+2+3 ⁴
ImageNet	ResNet-18 (69.69)	8/8	69.53	69.51	69.51	69.27	69.33	69.43
		6/6	67.19	67.90	68.44	67.19	67.95	68.46
		4/4	41.34	54.71	61.06	41.34	54.87	59.17
	MobileNetV2 (71.78)	8/8	69.86	70.84	71.23	71.01	70.92	71.25
		6/6	55.17	63.97	67.16	64.15	65.33	67.64
		4/4	2.70	13.46	14.61	7.08	15.58	25.35
CIFAR-10	ResNet-32 (92.63)	5/5	91.54	91.73	91.77	91.70	91.93	91.74
		4/4	89.02	89.02	89.69	89.03	89.71	90.24
		3/3	74.56	74.56	76.76	75.74	77.35	79.69

¹ 1st-order rounding scheme of Q-Rater

² 2nd-order rounding scheme of Q-Rater

³ Clipping method of Q-Rater

⁴ Bias Correction of Q-Rater

Table 3 summarizes the results of the 1st-order and the 2nd-order rounding scheme. The results with the 2nd-order scheme are the same as in Table 1. In general, the 2nd-order scheme results in better accuracy than the 1st-order scheme. Combined with the clipping method and the bias correction of Q-Rater, the accuracy can be further improved.

B. Evaluation of Q-Rater Clipping Methods

In this section, we evaluate the effectiveness of the proposed Q-Rater clipping methods over the ResNet-18 and the MobileNetV2 models. Both models used in the evaluation are trained on ImageNet dataset. In the paper, we introduced γ_c as a new hyper-parameter for the clipping. Note that γ_c ranges between 0.0 and 1.0. For the conventional scheme, we choose MSE minimization, ACIQ, and KL divergence minimization. For more details on the conventional methods, please refer to Section 5.2.

B.1. ResNet-18

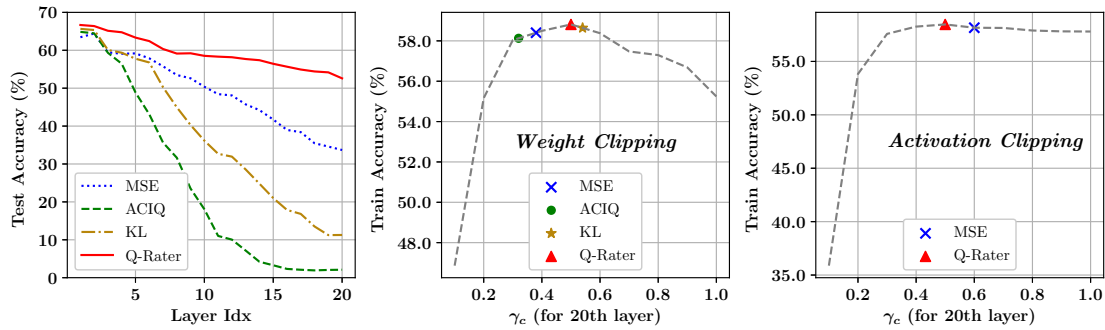


Figure 16. Comparison of different clipping methods with RTN rounding scheme. For quantization, 4 bits are used for both weights and activations.

Figure 16 compares different clipping methods with RTN rounding scheme in ResNet-18. The clipping and the quantization are performed per-layer incrementally as in the previous experiments. Thus, test accuracy drops as the layer index increases as in the leftmost figure. However, the proposed Q-Rater clipping method is remarkably tolerant in the accuracy drop compared to other schemes. Test accuracy with Q-Rater clipping and RTN rounding results in 55.48%. The second and the third plots show training accuracy by different γ_c applied in the weight clipping and the activation clipping respectively. Each clipping method calculates different γ_c with their own algorithms, but that does not necessarily result in the best accuracy. Based on the training accuracy, Q-Rater finds γ_c to achieve the best accuracy.

B.2. MobileNetV2

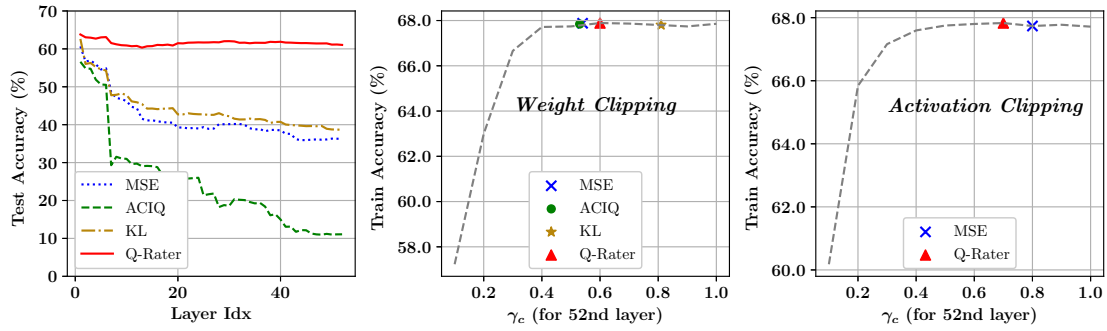


Figure 17. Test accuracy comparison using MSE, ACIQ, KL, or our proposed clipping method with RTN rounding scheme for weights and activations of MobileNetV2 model on ImageNet ($q = 6$ for both weights and activations).

Figure 17 compares different clipping methods with RTN rounding scheme in MobileNetV2. The clipping and the quantization are performed per-layer incrementally as in the previous experiments. The first plot indicates that Q-Rater significantly outperforms other clipping methods. The second and the third plots show train accuracy by different γ_c applied in the weight clipping and the activation clipping respectively. Note that Q-Rater clipping is applied until the 52nd layer. Only the last layer of the model is clipped with different clipping methods in the second and the third plot. Since the accuracy drop by different clipping schemes mostly occurs at the early layers, the difference of train accuracy among those clipping methods seems comparatively small.

C. Evaluation of Q-Rater Bias Correction Methods

In this section, we evaluate the effectiveness of the proposed Q-Rater bias correction methods over the ResNet-18 and the MobileNetV2 models. Both models used in the evaluation are trained on the ImageNet dataset. In Q-Rater, bias correction is applied per layer only when it improves train accuracy.

C.1. ResNet-18

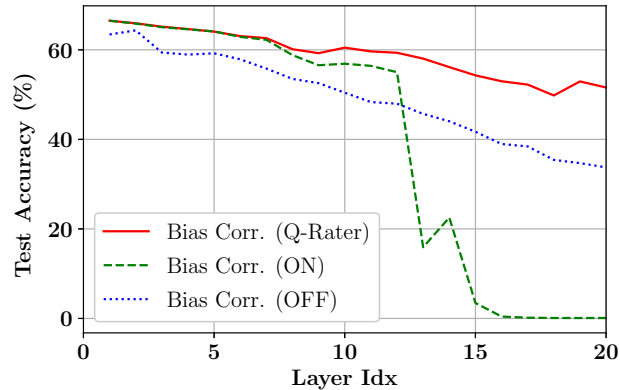


Figure 18. Test accuracy of ResNet-18 model on ImageNet when bias correction is always applied, never applied, or selectively applied by Q-Rater. Weights and activations are quantized using $q = 4$ incrementally with RTN and MSE clipping.

Figure 18 shows the test accuracy of ResNet-18 model trained on the ImageNet dataset. Interestingly, ResNet-18 shows the worst performance when bias correction is applied to all layers. Bias correction is supposed to compensate for the errors from quantization. However, the result indicates that minimizing quantization errors by bias correction may not lead to better performance. The result indicates Q-Rater effectively achieves the best performance by selectively enabling the bias correction per layer.

C.2. MobileNetV2

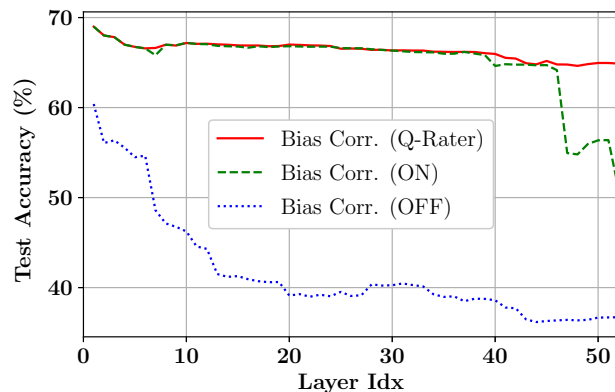


Figure 19. Test accuracy of MobileNetV2 model on ImageNet when bias correction is always applied, never applied, or selectively applied by Q-Rater. Weights and activations are quantized using $q = 6$ incrementally with RTN and MSE clipping.

Figure 19 shows the test accuracy of MobileNetV2 model trained on the ImageNet dataset. Although applying bias correction is effective on many layers, accuracy drops abruptly at the 40th layer and the 46th layer. We observed that weight values are biased and have high variance per channel at those layers. For example, the entire weights in some channels are negative, while the entire weights in other channels are all positive. In such cases, applying bias correction only adds

errors to both channels. The result indicates Q-Rater effectively achieves the best performance by selectively enabling the bias correction per layer.

C.3. Bias Correction Selection Results

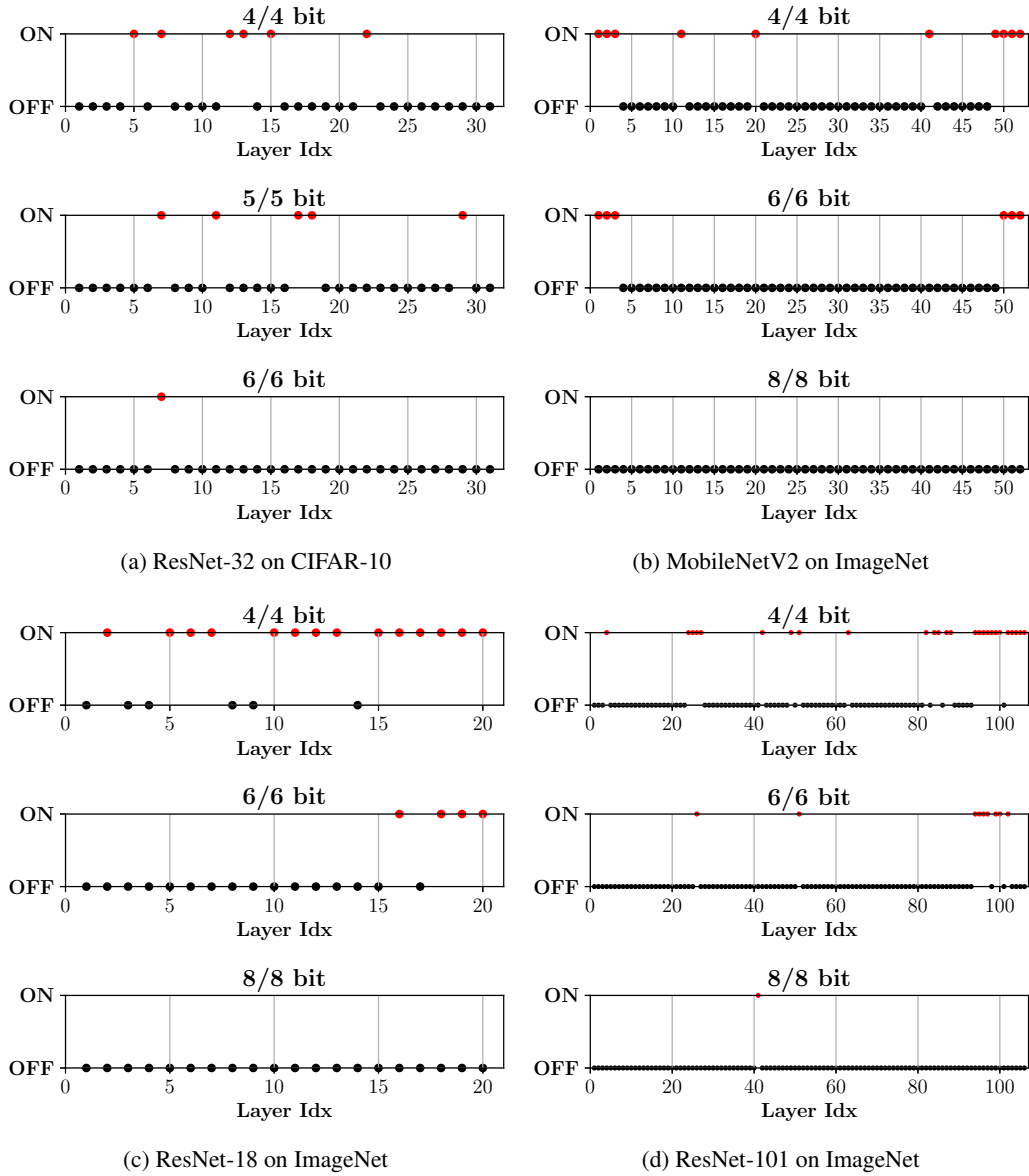


Figure 20. Bias correction On-Off patterns on different models.

Figure 20 presents which layers have been selected for the bias correction. Overall, our results do not show specific patterns on bias correction selections except for two observations: 1) when a model is quantized into lower bits, bias correction seems to be more effective because bias correction can compensate accumulated errors by quantization (e.g., bias correction is seldomly applied to 8-bit quantized models.) and 2) For quantized MobileNetV2 with 4/4 and 6/6 bits, it is effective to apply bias correction to a few layers close to inputs or outputs.

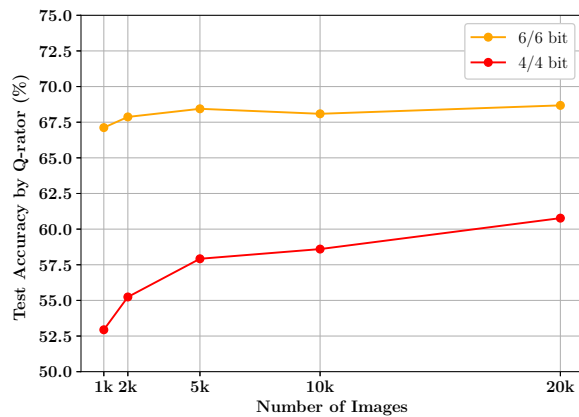


Figure 21. Test accuracy of ResNet18 model on ImageNet Nk is used.

D. The Impact of Calibration Set Size on ResNet-18 Quantization

For the experimental results in the main manuscript, we used 20k ImageNet dataset which consists of 20 randomly picked images per class from the original ImageNet dataset. Since using the whole dataset for hyper-parameter search (e.g., for m , s) is impractical and inefficient, we can select a dataset of small size if such a small dataset can exhibit a similar distribution of the original dataset. Figure 21 shows the test accuracy measured on ResNet18 model quantized by 4/4 and 6/6 bits while we increase the number of images per class. We observe that our selection (20 images per class in the main manuscript) is enough to obtain high test accuracy.

E. Algorithm Descriptions on Q-Rater Operations

In Algorithm 1, we provide pseudo-codes of the proposed Q-Rater algorithm. We briefly explain each function.

Run() Q-Rater executes Run() to quantize a model. For each layer, three functions are called to quantize weights, quantize activations, and perform bias correction.

WeightQuant(i) This function quantizes the weight values. Firstly, the original weight values are stored. And then, the function finds γ_c through Bayesian Optimization and performs clipping. When the weight clipping is finished, the function continues finding hyper-parameters for quantization: γ_n and γ_s . With the determined hyper-parameters, the function performs quantization.

WeightClip(w_{org}, γ_c, i) This function clips weight values for given γ_c . TH_c is calculated by multiplying γ_c and the maximum absolute value of weights.

WeightRound($w_c, s, \gamma_n, \gamma_s, i$) This function performs weight rounding with given hyper-parameters. For more details on the rounding equation, please refer to the paper, equation (2) for the 1st-order rounding and equation (4) for the 2nd-order rounding.

ActQuant(i) This function quantizes the activation values. Firstly, the function finds γ_c to perform activation clipping through ActClip function. When the activation clipping is done, the function finds γ_n and γ_s for quantization through Bayesian Optimization. With the determined hyper-parameters, the function performs activation quantization.

ActClip(γ_c, i) This function clips activation values for given γ_c . TH_c is calculated by multiplying γ_c and the maximum absolute value of activation.

ActRound(γ_n, γ_s, i) This function performs activation rounding with given hyper-parameters. For more details on the rounding equation, please refer to the paper, equation (2) for the 1st-order rounding and equation (4) for the 2nd-order rounding.

BiasCorr(i) This function performs bias correction. The function evaluates twice: with and without the bias correction. Finally, the function returns a better result.

Algorithm 1: Overall algorithm of Q-Rater

<p>M A target model</p> <p>$M.w^i$ A weight of the i^{th} layer</p> <p>$M.x_j^i$ An input of the i^{th} layer for the j^{th} batch</p> <p>N_{layer} The number of layers in M</p> <p>f_{eval} An evaluation function with quant. parameters</p> <p>S_x Scaling factors for each activation</p> <p>Γ_n, Γ_s γ_n and γ_s for each activation</p> <p>BC_x An indicating vector for bias-correction</p> <p>q The number of quantization bits</p> <p>BO Bayesian optimizer</p> <p>.probe registers a given point</p> <p>.run optimizes a function within given parameter ranges</p>	<p>Func WeightRound ($w, s, \gamma_n, \gamma_s, i$) :</p> <p style="padding-left: 20px;">$w' \leftarrow s \cdot \lfloor \frac{w}{s} + 0.5 + f_r(w, \gamma_n, \gamma_s) \rfloor \triangleright \text{Eq. (4)}$</p> <p style="padding-left: 20px;">$M.w_i \leftarrow w'$</p> <p style="padding-left: 20px;">return $f_{\text{eval}}(M, S_x, \Gamma_n, \Gamma_s, BC_x)$</p> <p>return</p>
<p>Func Run () :</p> <p style="padding-left: 20px;">for $i \leftarrow 1$ to N_{layer} do</p> <p style="padding-left: 40px;">WeightQuant (i)</p> <p style="padding-left: 40px;">ActQuant (i)</p> <p style="padding-left: 40px;">BiasCorr (i)</p> <p style="padding-left: 20px;">end</p> <p>return</p>	<p>Func ActQuant (i) :</p> <p style="padding-left: 20px;">for $\gamma_c \leftarrow 0.1$ to 1.0 by 0.1 do</p> <p style="padding-left: 40px;">$acc \leftarrow \text{ActClip}(\gamma_c, i)$</p> <p style="padding-left: 40px;">BO.probe(γ_c, acc)</p> <p style="padding-left: 20px;">end</p> <p style="padding-left: 20px;">$\gamma_c^* \leftarrow \text{BO.run}(\text{ActClip}, \gamma_c = (0, 1.0))$</p> <p style="padding-left: 20px;">$Th_c = (\sum_{j=1}^{n_{\text{batch}}} \gamma_c^* \times \max M.x_j^i) / n_{\text{batch}}$</p> <p style="padding-left: 20px;">$S_x^i = Th_c / (2^{q-1} - 1)$</p> <p style="padding-left: 20px;">for $\gamma_n \leftarrow -1.0$ to 1.0 by 0.1 do</p> <p style="padding-left: 40px;">for $\gamma_s \leftarrow 0.0$ to 1.0 by 0.25 do</p> <p style="padding-left: 60px;">$acc \leftarrow \text{ActRound}(\gamma_n, \gamma_s, i)$</p> <p style="padding-left: 60px;">BO.probe($(\gamma_n, \gamma_s), acc$)</p> <p style="padding-left: 40px;">end</p> <p style="padding-left: 20px;">end</p> <p style="padding-left: 20px;">$\gamma_n^*, \gamma_s^* \leftarrow \text{BO.run}(\text{ActRound},$</p> <p style="padding-left: 40px;">$\gamma_n = (-1.0, 1.0), \gamma_s = (0, 1.0))$</p> <p style="padding-left: 20px;">$\Gamma_n^i, \Gamma_s^i \leftarrow \gamma_n^*, \gamma_s^*$</p> <p>return</p>
<p>Func WeightQuant (i) :</p> <p style="padding-left: 20px;">$w_{\text{org}} \leftarrow M.w^i$</p> <p style="padding-left: 20px;">for $\gamma_c \leftarrow 0.1$ to 1.0 by 0.1 do</p> <p style="padding-left: 40px;">$acc \leftarrow \text{WeightClip}(w_{\text{org}}, \gamma_c, i)$</p> <p style="padding-left: 40px;">BO.probe(γ_c, acc)</p> <p style="padding-left: 20px;">end</p> <p style="padding-left: 20px;">$\gamma_c^* \leftarrow \text{BO.run}(\text{WeightClip}, \gamma_c = (0, 1.0))$</p> <p style="padding-left: 20px;">$Th_c \leftarrow \gamma_c^* \times \max(w_{\text{org}})$</p> <p style="padding-left: 20px;">$w_c \leftarrow \max(\min(w_{\text{org}}, Th_c), -Th_c)$</p> <p style="padding-left: 20px;">$s \leftarrow Th_c / (2^{q-1} - 1)$</p> <p style="padding-left: 20px;">for $\gamma_n \leftarrow -1.0$ to 1.0 by 0.1 do</p> <p style="padding-left: 40px;">for $\gamma_s \leftarrow 0.0$ to 1.0 by 0.25 do</p> <p style="padding-left: 60px;">$acc \leftarrow \text{WeightRound}(w_c, s, \gamma_n, \gamma_s, i)$</p> <p style="padding-left: 60px;">BO.probe($(\gamma_n, \gamma_s), acc$)</p> <p style="padding-left: 40px;">end</p> <p style="padding-left: 20px;">end</p> <p style="padding-left: 20px;">$\gamma_n^*, \gamma_s^* \leftarrow \text{BO.run}(\text{WeightRound},$</p> <p style="padding-left: 40px;">$\gamma_n = (-1.0, 1.0), \gamma_s = (0, 1.0))$</p> <p style="padding-left: 20px;">$M.w^i \leftarrow s \cdot \lfloor \frac{w_c}{s} + 0.5 + f_r(w_c, \gamma_n^*, \gamma_s^*) \rfloor$</p> <p>return</p>	<p>Func ActClip (γ_c, i) :</p> <p style="padding-left: 20px;">$Th_c = (\sum_{j=1}^{n_{\text{batch}}} \gamma_c \times \max M.x_j^i) / n_{\text{batch}}$</p> <p style="padding-left: 20px;">$S_x^i = Th_c / (2^{q-1} - 1)$</p> <p style="padding-left: 20px;">return $f_{\text{eval}}(M, S_x, \Gamma_n, \Gamma_s, BC_x)$</p> <p>return</p> <p>*Activation rounding is performed dynamically within evaluation function.</p> <p>Func ActRound (γ_n, γ_s, i) :</p> <p style="padding-left: 20px;">$\Gamma_n^i, \Gamma_s^i \leftarrow \gamma_n, \gamma_s$</p> <p style="padding-left: 20px;">return $f_{\text{eval}}(M, S_x, \Gamma_n, \Gamma_s, BC_x)$</p> <p>return</p>
<p>Func WeightClip (w, γ_c, i) :</p> <p style="padding-left: 20px;">$Th_c \leftarrow \gamma_c \times \max(w)$</p> <p style="padding-left: 20px;">$M.w_i \leftarrow \max(\min(w, Th_c), -Th_c)$</p> <p style="padding-left: 20px;">return $f_{\text{eval}}(M, S_x, \Gamma_n, \Gamma_s, BC_x)$</p> <p>return</p>	<p>Func BiasCorr (i) :</p> <p style="padding-left: 20px;">$acc^{off} \leftarrow f_{\text{eval}}(M, S_x, \Gamma_n, \Gamma_s, BC_x)$</p> <p style="padding-left: 20px;">$BC_x^i = TRUE$</p> <p style="padding-left: 20px;">$acc^{on} \leftarrow f_{\text{eval}}(M, S_x, \Gamma_n, \Gamma_s, BC_x)$</p> <p style="padding-left: 20px;">if $acc^{off} > acc^{on}$ then</p> <p style="padding-left: 40px;">$BC_x^i = FALSE$</p> <p style="padding-left: 20px;">end</p> <p>return</p>